

Bone Dimensions in the Posterior Mandible: A Retrospective Radiographic Study Using Cone Beam Computed Tomography. Part 2— Analysis of Edentulous Sites



Vedrana Braut, DDS, Dr Med Dent¹
Michael M. Bornstein, Prof Dr Med Dent²
Ulrike Kuchler, Dr Med, Dr Med Dent³
Daniel Buser, Prof Dr Med Dent⁴

A precise radiographic evaluation of the local bone dimensions and morphology is important for preoperative planning of implant placement. The purpose of this retrospective study was to analyze dimensions and morphology of edentulous sites in the posterior mandible using cone beam computed tomography (CBCT) images. This retrospective radiographic study measured the bone width (BW) of the mandible at three locations on CBCT scans for premolars (PM1, PM2) and molars (M1, M2): at 1 mm and 4 mm below the most cranial point of the alveolar crest (BW1, BW2) and at the superior border of the mandibular canal (BW3). Furthermore, the height (H) of the alveolar process (distance between the measuring points BW1 and BW3), as well as the presence of lingual undercuts, were analyzed. A total of 56 CBCTs met the inclusion criteria, resulting in a sample size of 127 cross sections. There was a statistically significant increase from PM1 to M2 for the BW2 ($P < .001$), which was not present for BW1 and BW3 values. For the height of the alveolar process, the values exhibited a decrease from PM1 to M2 sites. Sex was a statistically significant parameter for H ($P = .001$) and for BW1 ($P = .03$). Age was not a statistically significant parameter for bone width (BW1: $P = .37$; BW2: $P = .31$; BW3: $P = .51$) or for the height of the alveolar process ($P = .41$) in the posterior mandible. Overall, 73 (57.5%) edentulous sites were evaluated to be without visible lingual undercuts; 13 (10.2%) sites exhibited lingual undercuts classified as influential for implant placement. Precise evaluation of the alveolar crest by cross-sectional imaging is of great value to analyze vertical and buccolingual bone dimensions in different locations in the posterior mandible. In addition, CBCTs are valuable to diagnosing the presence of and potential problems caused by lingual undercuts prior to implant placement. (Int J Periodontics Restorative Dent 2014;34:639–647. doi: 10.11607/prd.1895)

¹ITI Scholar, Department of Oral Surgery and Stomatology, School of Dental Medicine, University of Bern, Bern, Switzerland; Assistant Lecturer, Department of Prosthodontics, School of Dental Medicine, Medical Faculty, University of Rijeka, Rijeka, Croatia.

²Associate Professor, Department of Oral Surgery and Stomatology, School of Dental Medicine, University of Bern, Bern, Switzerland.

³Resident, Department of Oral Surgery and Stomatology, School of Dental Medicine, University of Bern, Bern, Switzerland.

⁴Professor and Chairman, Department of Oral Surgery and Stomatology, School of Dental Medicine, University of Bern, Bern, Switzerland.

Correspondence to: Prof Dr Daniel Buser, Department of Oral Surgery and Stomatology, School of Dental Medicine, University of Bern, Freiburgstrasse 7, CH-3010 Bern, Switzerland; fax: +41 31 632 98 84; email: daniel.buser@zmk.unibe.ch.

The first and second authors contributed equally to this study.

©2014 by Quintessence Publishing Co Inc.

The long-term stability of a dental implant requires the presence of a buccal bone wall to provide circumferential bone anchorage in the crest area. Thus, the crest width at a potential implant site is an important parameter to be analyzed during preoperative analysis.¹ The second anatomical parameter of interest is the available bone height, which can be limited by anatomical structures such as the inferior alveolar nerve,² the floor of the maxillary

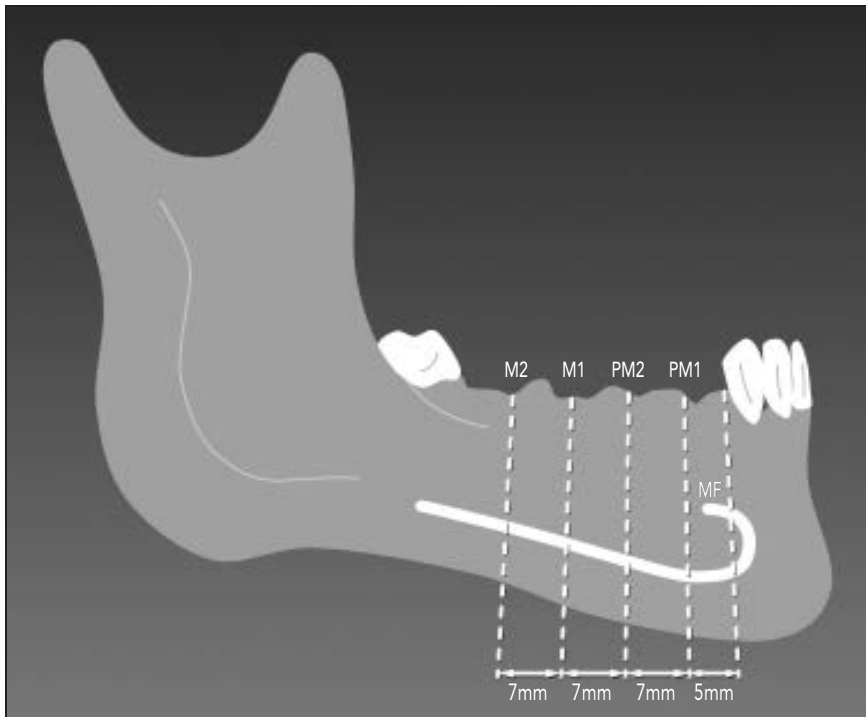


Fig 1 Evaluated cross-section locations at premolar (PM1, PM2) and molar (M1, M2) sites. Site 1 lies 5 mm distally to the first mesial tooth present. Sites 2, 3, and 4 are consecutively located 7 mm farther distally for distal extension situations. MF = mental foramen.

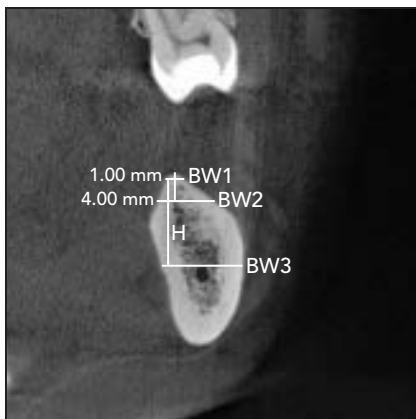


Fig 2 The alveolar bone width was measured at three locations: at 1 and 4 mm below the most cranial point of the alveolar crest (BW1 and BW2) and at the superior border of the mandibular canal (BW3). The height of the alveolar process (H) was defined as the distance between BW1 and BW3.

sinus,³ and the floor of the nose.⁴ For preoperative planning, precise radiographic evaluation of available bone volume and morphology is often necessary in addition to the clinical examination.⁵

Three-dimensional (3D) imaging modalities (computed tomography [CT] or cone beam CT [CBCT]) have become widely used in the field of dental medicine,⁶ especially for

preoperative planning of dental implant surgery, including bone quality assessment.^{5,7-10} These methods provide high-resolution 3D images, which are considered to be superior to panoramic images for detailed evaluation of mandibular size and morphology.¹¹ Today, CBCT is preferred over CT, because this new technology offers better image quality and lower radiation exposure.^{5,12}

The purpose of this retrospective radiographic study was to analyze the local bone dimensions of edentulous sites in the posterior mandible based on CBCT images from patients referred for dental implant planning and therapy. The results for dentate sites in the posterior mandible have already been reported in a previous publication.¹³

Method and materials

Patients

The study included all CBCT scans (3D Accuitomo XYZ Slice View Tomograph, Morita) with dentoalveolar fields of view (FOV; 4×4 , 6×6 , or 8×8 cm) from patients referred to the Department of Oral Surgery and Stomatology, School of Dental Medicine, University of Bern, Bern, Switzerland for implant therapy in the posterior mandible between January and December 2009.

Radiographic image analysis

CBCT images were analyzed on an Eizo Flexscan (Eizo) monitor with a resolution of $1,280 \times 1,024$ pixels. Data were reconstructed with slices of 1-mm (FOV: 4×4 and 6×6 cm) and 1.28-mm (FOV: 8×8 cm) thickness. To avoid artifacts from metallic restorations, the occlusal plane was always aligned horizontally. If artifacts made an analysis impossible, the respective areas were excluded from the present study.

Coronal sections of the CBCT scans were evaluated at premolar and molar sites for planning of the placement of a regular body dental implant: 5 mm distally to the first mesial tooth (eg, the canine) was defined as site 1. Following cross sections, consecutively located 7 mm farther distally, were defined as sites 2, 3, and 4 (Fig 1). In patients who had no mesial reference tooth, the cross-sectional image in which the mental foramen was recognized

was defined as site 1. The line representing the axis of the planned implant aiming toward the palatal cusp of the opposing tooth in the maxilla subsequently dictated the vertical orientation of the slice. To perform the measurements, coronal scans were displayed with the largest zoom factor possible. Image analysis was done with a digital sliding caliper using image processing software (i-Dixel, Morita).

The bone width (BW) of the mandible was measured at three locations on coronal CBCT slices (Fig 2): at 1 and 4 mm below the most cranial point of the alveolar crest (BW1 and BW2) and at the superior border or roof of the mandibular canal (BW3). In cases where the analyzed site was just above the mental foramen, the upper edge of the foramen was considered as the cranial border of the canal. The height of the alveolar process (H) was defined as the distance between BW1 and BW3 (see Fig 2). In addition, the presence of a lingual undercut above the mandibular canal was evaluated. Lingual undercuts were categorized into undercuts not influential and undercuts influential for implant placement (Fig 3). If the insertion of a standard implant with a length of 10 mm in the desired orofacial position and angulation would be prevented by the lingual undercut, it was classified as influential for implant placement.

Mandibular cross sections were further classified into two different morphologic categories based on the difference between BW2 and BW3 ($\Delta BW3-BW2$), represent-

ing the level of caudal divergence of the buccal and lingual cortical plates. Mandible cross sections with a $\Delta BW3-BW2 \leq 1$ mm were defined as type A, and cross sections with a $\Delta BW3-BW2 > 1$ mm were defined as type B (Fig 4).

All measurements were performed by a single examiner blinded to the clinical findings and follow-up of the included patients (VB). Presence of lingual undercuts in the edentulous space above the mandibular canal was additionally assessed by another examiner (UK). Each examiner evaluated the presence of lingual undercuts twice. In all cases of disagreement, a consensus was obtained by discussion between the two examiners.

Statistical analysis

All data were first analyzed descriptively. To detect significant differences in the data sets for the left and right sides of the maxilla, Wilcoxon signed rank tests for paired data were analyzed using exact *P* values. As there were no significant differences between data sets, the teeth were pooled into first premolar (PM1), second premolar (PM2), first molar (M1), and second molar (M2) groups for further statistical analysis. Kruskal-Wallis and non-parametric analysis of variance (ANOVA) tests using the method described by Brunner et al¹⁴ were applied to evaluate the influence of age, sex, and tooth location. To detect differences between the distribution of lingual undercuts, a chi-square test was applied. To analyze

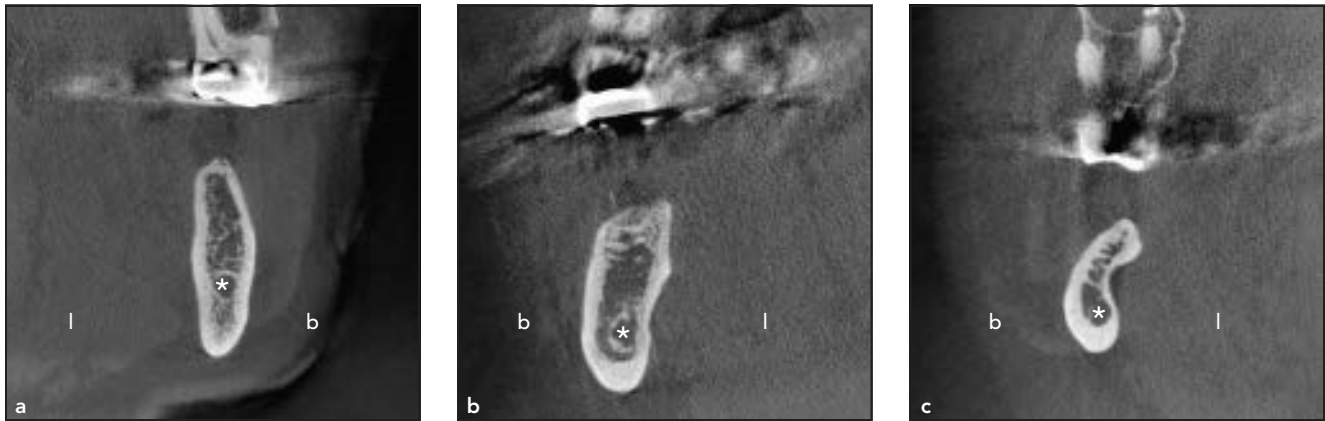


Fig 3 Presence of a lingual undercut above the mandibular canal. (a) Lingual undercut not present. (b) Lingual undercut present but not influential for implant placement. (c) Lingual undercut present and influential for implant placement, preventing the insertion of a standard 10-mm dental implant in the desired orofacial position. l = lingual aspect; b = buccal aspect; * = mandibular canal.

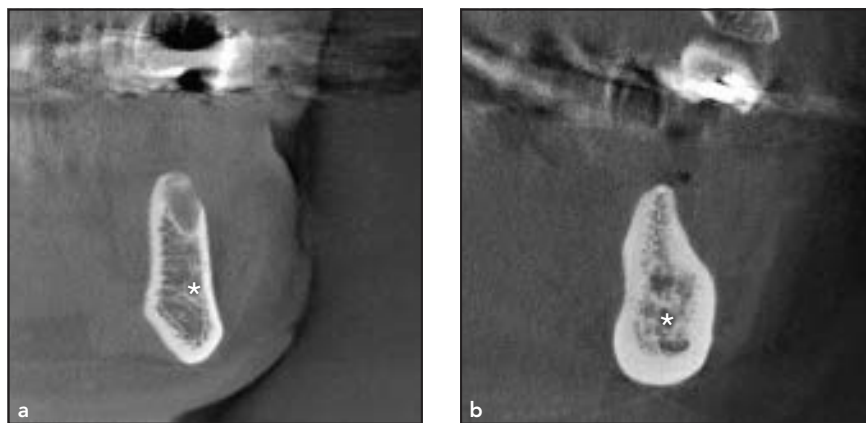


Fig 4 Categories of mandibular shapes as classified based on coronal CBCT scans. * = mandibular canal. (a) Type A mandible cross section ($\Delta BW3-BW2 \leq 1$ mm). (b) Type B cross section ($\Delta BW3-BW2 > 1$ mm).

Table 1 Distribution of the analyzed potential dental implant sites in the posterior mandible from 127 CBCT cross sections analyzed (56 patients)

	Potential implant site*								Total
	47	46	45	44	34	35	36	37	
n (analyzed)	15	24	16	7	9	22	18	16	127

*Federation Dentaire Internationale tooth-numbering system.

the consistency of the intra- and interrater observations, Cohen kappa values were calculated. For the statistical analysis the internet-based

R software package (R 2.7.1) was used. The ANOVA tests were performed using a licensed software package (SAS 9.1, SAS Institute).

Results

The sample consisted of 56 patients (22 men and 34 women) with a mean age of 54.5 years (range: 17 to 82 years), resulting in a sample size of 127 cross sections of potential implant sites. Distribution of the analyzed potential implant sites is presented in Table 1.

Width of the alveolar crest

For the bone width at 1 mm below the most cranial point of the alveolar crest (BW1) and at the cranial border of the mandibular canal (BW3), there were no statistically significant differences for premolar and molar locations ($P = .78$ for BW1; $P = .10$ for BW3; Table 2 and Fig 5). There was a statistically significant increase from PM1 to M2 for BW2 ($P < .001$; see Table 2 and Fig 5).

Regarding the morphologic type of the alveolar crest in different locations of the posterior mandible, type A was more frequently

found in molar sites than in premolar sites, whereas type B was most frequently seen in PM1 sites ($P = .01$; Table 3). This indicates that the BW2 values were generally lower in relation to BW3 values for edentulous premolar sites.

Sex was a statistically significant parameter for BW1 ($P = .03$), with male patients exhibiting higher values than female patients. BW2 exhibited a borderline significance ($P = .07$), and for BW3 there was no statistically significant difference between the sexes ($P = .21$). Age was not a statistically significant parameter for bone width (BW1: $P = .37$; BW2: $P = .31$; BW3: $P = .51$).

Height of the alveolar process

For the bone height above the mandibular canal, there were statistically significant differences for premolar and molar sites ($P = .02$; Fig 6; see Table 2). The values exhibited a steady decrease from PM1 to M2. Sex was a statistically significant parameter for the height of the alveolar process ($P = .001$), with male patients exhibiting higher values than female patients. Age was not a statistically significant parameter for height in the posterior mandible ($P = .41$).

Lingual undercuts

Overall, 73 (57.5%) edentulous sites showed no lingual undercuts, and 54 (42.5%) had lingual undercuts, 13 (10.2%) of which were classified as influential for the placement of

Group	Minimum	Median	Mean	Maximum	Teeth (n)
BW1					
PM1	2.380	3.245	3.473	5.750	16
PM2	0.750	3.280	3.596	10.750	38
M1	1.120	3.305	4.056	11.360	42
M2	1.380	3.575	3.689	6.560	30
BW2					
PM1	3.250	5.500	5.667	8.000	16
PM2	2.880	6.450	6.126	10.880	38
M1	3.630	7.815	7.652	12.640	42
M2	4.750	8.240	8.604	13.440	30
BW3					
PM1	6.000	8.820	9.064	12.480	16
PM2	5.380	8.205	8.910	13.760	38
M1	6.630	9.330	9.806	15.680	42
M2	5.380	9.690	10.100	16.640	30
H					
PM1	9.750	15.220	15.160	22.130	16
PM2	6.240	13.320	13.320	21.250	38
M1	5.750	12.570	12.470	20.500	42
M2	7.360	11.800	11.930	19.250	30

Alveolar crest morphology	PM1 sites		PM2 sites		M1 sites		M2 sites	
	n	%	n	%	n	%	n	%
Type A	2	12.50	12	31.58	11	26.19	14	46.67
Type B	14	87.50	26	68.42	31	73.81	16	53.33

Type A = Δ (BW3-BW2) \leq 1 mm; Type B = Δ (BW3-BW2) $>$ 1 mm.

dental implants (Table 4). There was a statistically significant difference, with molars exhibiting more undercuts than premolars ($P < .001$). All lingual undercuts potentially influ-

encing dental implant placement were found at either M1 or M2 positions (Table 4).

The analysis of the consistency of the observers' rating of lingual

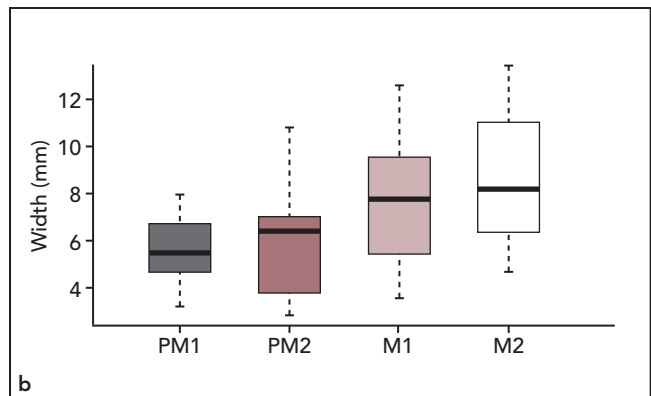
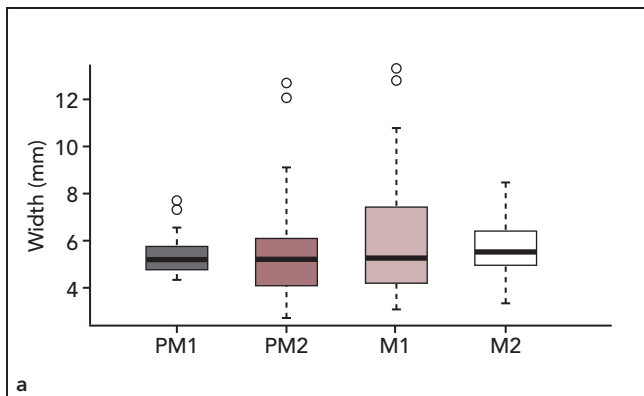


Fig 5 Box plots demonstrating the distribution of the alveolar crest width at (a) BW1, (b) BW2, and (c) BW3 at different potential implant sites in the posterior mandible. ° = outlier values.

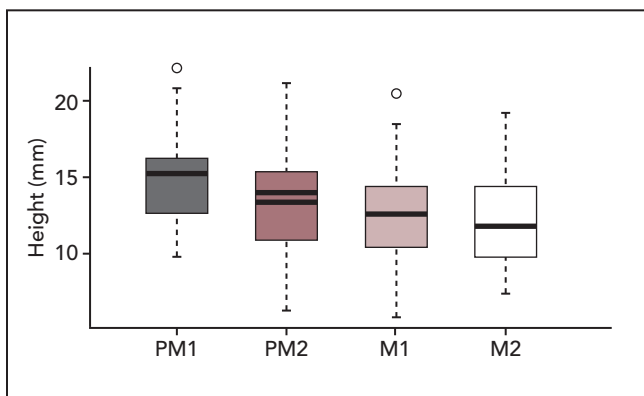
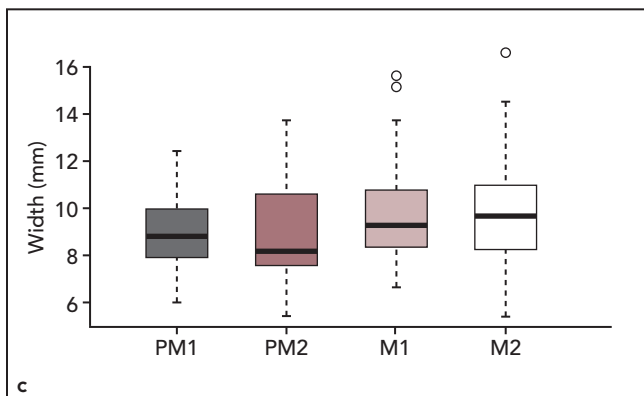


Fig 6 Box plot demonstrating the distribution of the alveolar crest height at different potential implant sites in the posterior mandible. ° = outlier values.

undercuts yielded high kappa values. Intraobserver reliability resulted in Cohen kappa values of 0.969 and 0.966, respectively. The interobserver values were 0.816 for comparison of the first set of analyses and 0.878 for comparison of the second set of analyses.

Discussion

The placement of dental implants in the posterior mandible in partially edentulous patients is a frequent intervention.¹⁵ In addition to the vertical height, bone morphology and dimensions in the orofacial and

mesiodistal directions are of importance for implant placement.¹⁶ Bone dimensions of the posterior mandible have been evaluated using different radiographic methods in several studies.^{11,17–20} However, in the majority of those studies imaging was not based on CBCT. Studies

Table 4 Distribution of the lingual undercuts at different potential implant sites in the posterior mandible

Lingual undercut status	PM1 sites		PM2 sites		M1 sites		M2 sites		Overall	
	n	%	n	%	n	%	n	%	n	%
No lingual undercuts	13	10.2	31	24.4	21	16.5	8	6.3	73	57.5
Noninfluential undercut	3	2.4	7	5.5	16	12.6	15	11.8	41	32.3
Influential undercut	0	0.0	0	0.0	4	3.1	9	7.1	13	10.2

analyzing CBCT images of the posterior mandible were done either on fully dentate subjects²¹ or were cadaveric studies^{20,22} focusing mainly on the accuracy of CBCT measurements.

In the present study, the mean alveolar crest width at 4 mm below the alveolar crest (BW2) ranged from 5.7 mm (PM1 sites) to 8.6 mm (M2 sites). These results are in line with a cadaveric study by Katranji and coworkers²² that reported mandibular width values at 3 mm below the alveolar crest ranging from 4.8 to 6.0 mm for premolar and molar sites, respectively. The results of the present study are also in line with another study¹⁶ that reported a gradual increase of the alveolar crest width above the mental foramen (corresponding to the crest width at 4 mm below the alveolar crest [BW2]) through the posterior region in contrast to the width at the lower border of the mental foramen, where the width values showed no statistically significant change.

In the present study, the height of the alveolar process ranged from 15.1 mm (first premolar sites) to 11.9 mm (second molar sites). Similar values have been reported

by another study²⁰ for the height of the alveolar process in the posterior mandible. This trend is in line with findings reported by Watanabe et al,¹⁶ although the study measured the distance between the superior border of the alveolar crest to the inferior border of the mandible. Bolin and coworkers¹⁸ analyzed panoramic images and also reported the height of the alveolar process in the posterior mandible to be greater in premolar compared with molar sites. The data from the present study are also in line with the known position of the mental foramen that has been reported to be located apically between the first and second premolars in two recent studies using CBCT imaging.^{23,24}

Knowledge of the exact location and course of the mandibular canal is of great importance to avoid neurosensory disturbances following placement of dental implants. In general, damage to sensory nerves can result in anesthesia, dysesthesia, pain, or a combination of these states.²⁵ Renton et al^{26,27} reported that the most important reason for this complication was proximity of the implant or implant bed preparation to the inferior alveolar canal, with a fifth of the re-

ported complication cases entering the canal, a fifth crossing the canal, and almost half contacting the roof of the canal.

Perforation of the lingual cortical plate during implant placement in the posterior mandible can be a severe surgical complication, and the presence of a lingual undercut is considered an important anatomical risk factor.²⁸ In the present study, 54 (42.5%) edentulous sites exhibited lingual undercuts, but only 13 (10.2%) were classified as potentially influential for dental implant placement (see Table 4). To assess the consistency of these potentially subjective ratings, intra- and interobserver reliability was evaluated and exhibited high Cohen kappa values ranging between 0.816 to 0.969. Molars tended to have more undercuts than premolars ($P < .001$). Presence of a lingual undercut above the mandibular canal was analyzed in dentate sites in a previous study¹³ and was observed in 38.93%.

When the minimal crest width to insert implants with a diameter of 4 or 5 mm is not available, the surgeon has the option to perform a local bone augmentation using guided bone regeneration (GBR)

or reduce the crest in height to increase the crest width. The present study showed that the majority of sites demonstrated an increase of crest width in an apical direction and measured clearly more than 6 mm at 4 mm below the alveolar crest (BW2) in molar regions, which allows for the placement of at least a 4-mm-diameter implant. The reported success of short (6- or 8-mm) implants,^{29,30} combined with the present data demonstrating increased ridge width at 1 (BW1) and 4 mm (BW2) below the alveolar crest, gives the implant surgeon the option of ridge reduction procedures as an alternative to GBR.

Conclusions

Regarding the data of the present study, precise evaluation of the alveolar crest by cross-sectional imaging is of great value to analyze vertical and orofacial bone dimensions in different locations in the posterior mandible prior to dental implant placement. Furthermore, the presence and potential problems caused by lingual undercuts can be estimated. Whether 3D radiographic assessment of potential implant sites in the posterior mandible results in fewer complications, such as neurovascular disturbances, or higher survival and success rates of dental implants, has to be addressed by future prospective and comparative clinical studies.

Acknowledgments

The authors thank Lukas Martig and Janine Kuratli, Institute of Mathematical Statistics and Actuarial Science, University of Bern, for their assistance during the statistical analysis. The authors reported no conflicts of interest related to this study.

References

- Buser D, von Arx T. Surgical procedures in partially edentulous patients with ITI implants. *Clin Oral Implants Res* 2000; 11(suppl 1):83–100.
- Grant BT, Pancko FX, Kraut RA. Outcomes of placing short dental implants in the posterior mandible: A retrospective study of 124 cases. *J Oral Maxillofac Surg* 2009;67:713–717.
- Nunes LS, Bornstein MM, Sendi P, Buser D. Anatomical characteristics and dimensions of edentulous sites in the posterior maxillae of patients referred for implant therapy. *Int J Periodontics Restorative Dent* 2013;33:337–345.
- Mazor Z, Lorean A, Mijiritsky E, Levin L. Nasal floor elevation combined with dental implant placement. *Clin Implant Dent Relat Res* 2012;14:768–771.
- Harris D, Horner K, Grondahl K, et al. E.A.O. guidelines for the use of diagnostic imaging in implant dentistry 2011. A consensus workshop organized by the European Association for Osseointegration at the Medical University of Warsaw. *Clin Oral Implants Res* 2012;23: 1243–1253.
- Ziegler CM, Woertche R, Brief J, Hassfeld S. Clinical indications for digital volume tomography in oral and maxillofacial surgery. *Dentomaxillofac Radiol* 2002;31: 126–130.
- Guerrero ME, Jacobs R, Loubele M, Schutyser F, Suetens P, van Steenberghe D. State-of-the-art on cone beam CT imaging for preoperative planning of implant placement. *Clin Oral Investig* 2006; 10:1–7.
- Kan JY, Roe P, Rungcharassaeng K, et al. Classification of sagittal root position in relation to the anterior maxillary osseous housing for immediate implant placement: A cone beam computed tomography study. *Int J Oral Maxillofac Implants* 2011;26:873–876.
- Nackaerts O, Maes F, Yan H, Couto Souza P, Pauwels R, Jacobs R. Analysis of intensity variability in multislice and cone beam computed tomography. *Clin Oral Implants Res* 2011;22:873–879.
- Pauwels R, Nackaerts O, Bellaiche N, et al. Variability of dental cone beam CT grey values for density estimations. *Br J Radiol* 2013;86:20120135.
- Quiryneen M, Mraiwa N, Van Steenberghe D, Jacobs R. Morphology and dimensions of the mandibular jaw bone in the interforaminal region in patients requiring implants in the distal areas. *Clin Oral Implants Res* 2003;14:280–285.
- Hirsch E, Wolf U, Heinicke F, Silva MA. Dosimetry of the cone beam computed tomography Veraviewepocs 3D compared with the 3D Accutomo in different fields of view. *Dentomaxillofac Radiol* 2008; 37:268–273.
- Braut V, Bornstein MM, Lauber R, Buser D. Bone dimensions in the posterior mandible: A retrospective radiographic study using cone beam computed tomography. Part 1—Analysis of dentate sites. *Int J Periodontics Restorative Dent* 2012; 32:175–184.
- Brunner E, Domhof S, Langer F. Non-parametric Analysis of Longitudinal Data in Factorial Experiments. New York: Wiley, 2002.
- Bornstein MM, Halbritter S, Harnisch H, Weber HP, Buser D. A retrospective analysis of patients referred for implant placement to a specialty clinic: Indications, surgical procedures, and early failures. *Int J Oral Maxillofac Implants* 2008;23: 1109–1116.
- Watanabe H, Mohammad Abdul M, Kurabayashi T, Aoki H. Mandible size and morphology determined with CT on a premise of dental implant operation. *Surg Radiol Anat* 2010;32:343–349.
- Lindh C, Petersson A, Klinge B. Measurements of distances related to the mandibular canal in radiographs. *Clin Oral Implants Res* 1995;6:96–103.
- Bolin A, Eliasson S, von Beetzen M, Jansson L. Radiographic evaluation of mandibular posterior implant sites: Correlation between panoramic and tomographic determinations. *Clin Oral Implants Res* 1996;7:354–359.
- Tepper G, Hofschneider UB, Gahleitner A, Ulm C. Computed tomographic diagnosis and localization of bone canals in the mandibular interforaminal region for prevention of bleeding complications during implant surgery. *Int J Oral Maxillofac Implants* 2001;16:68–72.

20. Kamburoglu K, Kilic C, Ozen T, Yuksel SP. Measurements of mandibular canal region obtained by cone-beam computed tomography: A cadaveric study. *Oral Surg Oral Med Oral Pathol Oral Radiol Endod* 2009;107:e34–42.
21. Swasty D, Lee JS, Huang JC, Maki K, Gansky SA, Hatcher D, et al. Anthropometric analysis of the human mandibular cortical bone as assessed by cone-beam computed tomography. *J Oral Maxillofac Surg* 2009;67:491–500.
22. Katranji A, Misch K, Wang HL. Cortical bone thickness in dentate and edentulous human cadavers. *J Periodontol* 2007;78:874–878.
23. Kalender A, Orhan K, Aksoy U. Evaluation of the mental foramen and accessory mental foramen in Turkish patients using cone-beam computed tomography images reconstructed from a volumetric rendering program. *Clin Anat* 2012;25:584–592.
24. von Arx T, Friedli M, Sendi P, Lozanoff S, Bornstein MM. Location and dimensions of the mental foramen: A radiographic analysis by using cone-beam computed tomography. *J Endod* 2013;39:1522–1528.
25. Jacobs R, Quirynen M, Bornstein MM. Neurovascular disturbances after implant surgery. *Periodontol* 2000 (in press).
26. Renton T, Dawood A, Shah A, Searson L, Yilmaz Z. Post-implant neuropathy of the trigeminal nerve. A case series. *Br Dent J* 2012;212:E17.
27. Renton T, Yilmaz Z. Profiling of patients presenting with posttraumatic neuropathy of the trigeminal nerve. *J Orofac Pain* 2011;25:333–344.
28. Chan HL, Benavides E, Yeh CY, Fu JH, Rudek IE, Wang HL. Risk assessment of lingual plate perforation in posterior mandibular region: A virtual implant placement study using cone beam computed tomography. *J Periodontol* 2011;82:129–135.
29. Renouard F, Nisand D. Impact of implant length and diameter on survival rates. *Clin Oral Implants Res* 2006;17(suppl 2):35–51.
30. Srinivasan M, Vazquez L, Rieder P, Moraguez O, Bernard JP, Belser UC. Efficacy and predictability of short dental implants (<8 mm): A critical appraisal of the recent literature. *Int J Oral Maxillofac Implants* 2012;27:1429–1437.